Porphyrinoids

Deutsche Ausgabe: DOI: 10.1002/ange.201500732
Internationale Ausgabe: DOI: 10.1002/anie.201500732

Phenanthriporphyrin: An Antiaromatic Aceneporphyrinoid as a Ligand for a Hypervalent Organophosphorus(V) Moiety**

*Bartosz Szyszko, Agata Białońska, Ludmiła Szterenberg, and Lechosław Latos-Grażyński**

Abstract: *The incorporation of a phenanthrene moiety into a porphyrin framework results in the formation of a hybrid macrocycle—phenanthriporphyrin—merging the structural features of polycyclic aromatic hydrocarbons and porphyrins. An antiaromatic aceneporphyrinoid, adopting the trianionic {CCNN} core, is suitable for the incorporation of a phosphorus(V) center to form a hypervalent organophosphorus(V) derivative.*

The redesign of the archetypical porphyrin frame realized through the replacement of pyrrolic ring(s) with other heterocycle(s) or carbocycle(s) creates innovative routes for the exploration of coordination and organometallic chemistry confined in a macrocyclic environment. Molecules comprising structural features of polycyclic aromatic hydrocarbons and polypyrrolic macrocycles in a manner which allows for electronic communication, for example aceneporphyrinoids, exemplify this approach.[1–10] Such compounds can demonstrate peculiar electronic and molecular structures and create a unique macrocyclic environment for coordination forcing atypical intermolecular reactivity. For instance, a contraction of *p*-phenylene to cyclopentadiene is triggered by insertion of palladium(II) or gold(III) into *p*-benziporphyrin.[6,11,12]

Herein, we report the synthesis and properties of a new member of the aceneporphyrinoid class, namely phenanthriporphyrin **4**-H_3 (Scheme 1). Formally, **4**-H_3 can be classified as a dicarbaporphyrinoid,[13,14] that is, as a porphyrinoid with two carbon atoms in the core {CCNN}, but also as a prototypical system containing the rigid phenathrenylene unit. In this contribution, we demonstrate that **4**-H_3 may act as a ligand for phosphorus(V) to form the organophosphorus derivative **4**-$P(OMe)_2$.

The preparation of **4**-H_3 required the synthesis of a suitable precursor allowing eventually the incorporation of a phenanthrene moiety into the macrocyclic structure. The synthetic route, summarized in Scheme 1, includes benzoylation of synthetically available 9,10-dimethoxyphenanthrene following the procedure reported previously for the diacetyl derivative to form 3,6-dibenzoyl-9,10-dimethoxyphenantrene (**1**).[32] The reduction of **1** with sodium borohydride yielded the diol **2** which was subsequently subjected to condensation with an excess of pyrrole according to related procedures to form phenanthritripyrrane **3**.[6,8,15] The condensation of **3** with benzaldehyde was undertaken using the conditions reported by Lindsey et al.[16] and the subsequent product was oxidized using 2,3-dichloro-5,6-dicyano-1,4-benzoquinone (DDQ) to form **4**-H_3, which, after chromatographic work-up and recrystallization, was isolated in 16% yield.

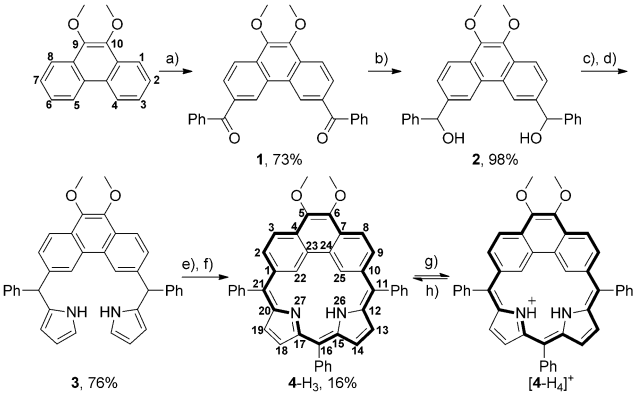

Scheme 1. Synthesis of **4**-H_3. Reaction conditions: a) PhCOCl (16.8 equiv), $AlCl_3$, DCE, 24 h; b) $NaBH_4$ (2.2 equiv), CH_2Cl_2, MeOH, 2 h; c) pyrrole (66 equiv), $Et_2O{:}BF_3$, reflux, 17 h; d) TEA; e) PhCHO (1 equiv), $Et_2O{:}BF_3$, CH_2Cl_2, 2 h; f) DDQ (2 equiv), g) TFA or HCl; h) TEA. DCE = 1,2-dichloroethane; TEA = triethylamine; TFA = trifluoroacetic acid.

When dissolved in chlorinated solvents, **4**-H_3 forms vividly green-colored solutions. Its UV/Vis absorption spectrum (Figure 1) consists of a narrow and intense band at $\lambda =$ 364 nm and a weak and broad absorption band that extends between $\lambda = 500$ and 1000 nm with a maximum at 816 nm. This absorption profile reflects an effective macrocyclic π delocalization.

The ^{1}H NMR spectrum of **4**-H_3 at 300 K reflects the effective C_{2v} symmetry of the molecule and is consistent with the macrocyclic structure of **4**-H_3 as being built of a 9,10-dimethoxyphenanthrene moiety linked with a *meso*-phenyldipyrromethene unit through two phenylmethine bridges (Figure 2 A). There is a distinct difference between the chemical shifts of the internally located (H(22,25): $\delta =$ 16.70 ppm) and externally located (H(2,9): $\delta = 5.94$ ppm) hydrogen atoms, expressed quantitatively by a $\Delta\delta$ value equal to 10.76 ppm, which clearly indicates the marked paratropicity. The broad line at $\delta = 16.70$ ppm (half-width of circa 50 Hz at 300 K) has been assigned to the overlapped H(22,25) and NH resonances. The significant deshielding of the N(26)H

[*] Dr. B. Szyszko, Dr. A. Białońska, Dr. L. Szterenberg, Prof. Dr. L. Latos-Grażyński
Department of Chemistry, University of Wrocław
14 F. Joliot-Curie St., 50-383 Wrocław (Poland)
E-mail: lechoslaw.latos-grazynski@chem.uni.wroc.pl
Homepage: http://llg.chem.uni.wroc.pl

[**] Financial support from the National Science Centre (Grants 2011/01/N/ST5/02557 and 2012/04A/ST5/00593) is kindly acknowledged. DFT calculations were carried out at the Poznań Supercomputer Center.

Supporting information for this article is available on the WWW under http://dx.doi.org/10.1002/anie.201500732.

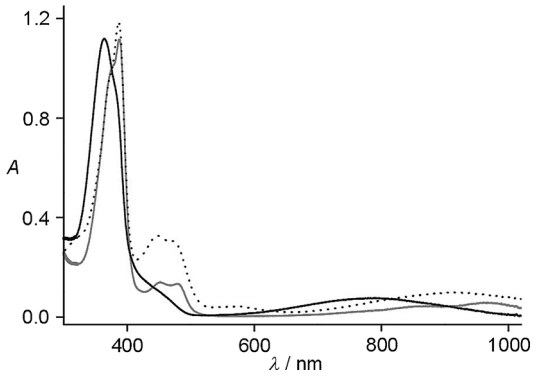

Figure 1. UV/Vis absorption spectra of **4**-H_3 (black solid line), [**4**-H_4]Cl (dotted line), and **4**-$P(OMe)_2$ (gray solid line) in solution in dichloromethane at 298 K.

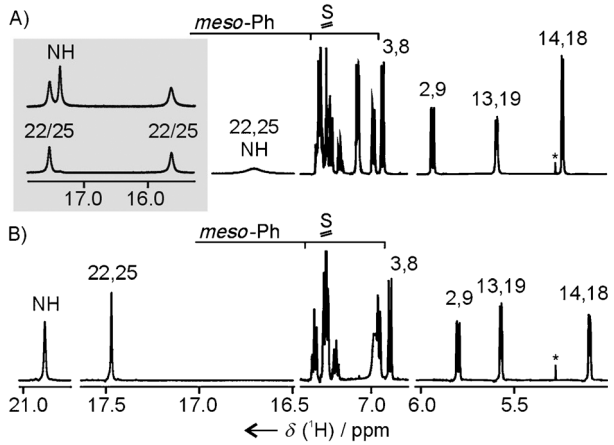

Figure 2. ^{1}H NMR spectra of A) **4**-H_3 (600 MHz, [D]chloroform, 300 K) and B) [**4**-H_4]Cl (500 MHz, [D]chloroform, 298 K). 5,6-OCH_3 signals have been omitted for clarity. Inset in trace (A) shows the most downfield region at the slow exchange limit (600 MHz, 170 K, [D_2]dichloromethane) before (top) and after (bottom) selective NH deuteration. S and * denote the residual solvent and dichloromethane peaks, respectively.

signal is a direct consequence of molecular antiaromaticity presumably strengthened by hydrogen bonding inside the N(26)–H–N(27) system.

The antiaromaticity of **4**-H_3 is illustrated by the chemical shifts attributable to phenanthrene protons which range from $\delta = 16.70$ ppm for an internally located H(22,25) hydrogen, through to $\delta = 6.94$ ppm for H(3,8) to $\delta = 5.94$ ppm for the H(2,9) signal (Figure 2 A). Accordingly, the chemical shifts of perimeter pyrrolic protons equal $\delta = 5.59$ ppm for H(13,19) and 5.24 ppm for H(14,18). Additionally, the order of signals of *meso*-phenyl protons is reversed in comparison to aromatic aceneporphyrinoids.[1,5,6] The antiaromaticity of **4**-H_3 is in contrast to the nonaromatic behavior of 1,10-phenanthroline-embedded porphyrin.[17]

The appearance of only four signals attributable to the dimethoxyphenanthrene moiety and one AB spin system for β-pyrrolic protons in the ^{1}H NMR spectrum ([D]chloroform, 300 K) confirms that **4**-H_3 tautomerizes rapidly on the NMR timescale, although the NH and H(22,25) broad resonances are indicative of the intermediate exchange rate (Figure 2 A). The process engages two equivalent tautomers through the exchange of the inner NH proton and involves two pyrrole nitrogen atoms. The variable-temperature (VT) studies demonstrated that the exchange processes slow down sufficiently at low temperature. Thus lowering of temperature to 170 K ([D_2]dichloromethane) resulted in doubling of the β-H resonances and systematic broadening of the H(2,9), H(3,8), and 5,6-methoxy signals (see Figures S11 and S12 in the Supporting Information). Three well-defined resonances eventually emerged at 170 K, have been assigned to the H(22/25) ($\delta = 17.52$ and 15.62 ppm) and NH ($\delta = 17.36$ ppm) protons.

The acidification of **4**-H_3 in dichloromethane with gaseous hydrochloride or trifluoroacetic acid (TFA) is accompanied by a color change from green to orange-green (orange in higher dilutions). The UV/Vis electronic spectrum of [**4**-H_4]Cl is similar to that of free base although in addition to an intense signal at $\lambda = 386$ nm and a broad absorption between 680–1000 nm with maximum at 909 nm a further three bands appear at 448, 469, and 576 nm (Figure 1).

The ^{1}H NMR spectrum of phenanthriporphyrin hydrochloride [**4**-H_4]Cl resembles that of **4**-H_3 (Figure 2 B). Two characteristic signals are present at $\delta = 20.57$ and 17.42 ppm which were assigned to N(26,27)H and H(22,25) protons, respectively. Applying the classical approach to account for the detected paratropicity, it is necessary to include the fundamental resonance contributors in the description of **4**-H_3 as shown at Scheme 2. Thus the structure **4**-H_3-1 defines

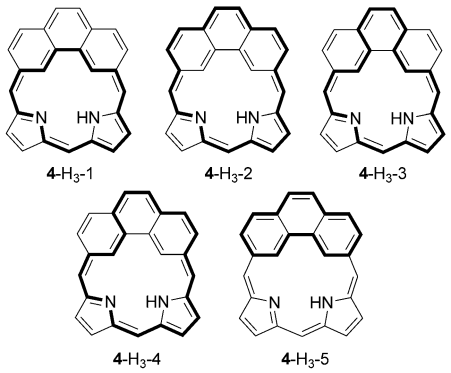

Scheme 2. Representative mesomers and π-delocalization pathways for **4**-H_3.

a 16-π-electron macrocyclic delocalization pathway which may coexist or compete with the 20-π-electron macrocyclic delocalization pathways of **4**-H_3-2, **4**-H_3-3, and **4**-H_3-4. In principle, the outlined delocalization routes can be realized in hypothetical [16]diphyrins(8.1) and [20]diphyrins(12.1). In contrast, the participation of an isolated [14]annulene system of phenanthrene, as marked in **4**-H_3-5, prohibits an overall macrocyclic π delocalization and, once dominating, is expected to impose the local phenanthrene-like aromaticity on the molecule and to affect appropriate spectroscopic properties.

In the solid state $[\mathbf{4}\text{-}H_4]^+$ adopts a folded conformation (Figure 3).[18] The folding is supplemented by the bowl-shape deformation of the phenanthrene subunit as reflected by the

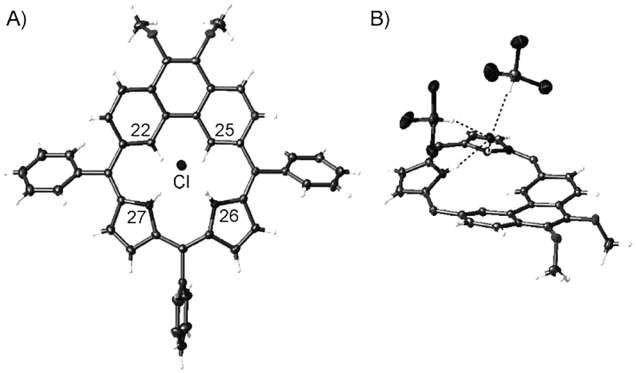

Figure 3. Molecular structure of $[\mathbf{4}\text{-}H_4]Cl$. In (B), the phenyl substituents at positions 11, 16, and 21 (see Scheme 1 for numbering scheme) are omitted for clarity. The chloride anion interacts through hydrogen bonds with two chloroform molecules. Selected bond lengths in [Å]: N(26)*H*—Cl 2.25(5), N(27)*H*—Cl 2.25(4), C*H*(chloroform)—Cl 2.27–2.50.

21.31(14)° dihedral angle between the planes of the terminal benzene rings of phenanthrene. The distortion from planarity reduces steric repulsions of inner CH and NH hydrogen atoms. Additionally, the geometry is stabilized by hydrogen bonds between NH donors and a chloride anion located 2.634(3) Å above the plane of three *meso* carbon atoms. The {CCNN} core of $[\mathbf{4}\text{-}H_4]^+$ is trapezoidal and comparable in both size and shape to those of corroles.[19] The carbon–carbon bond lengths of the phenanthrene unit resemble closely those reported for 9,10-dihydroxyphenanthrene.[20] The geometry of the dipyrromethene unit in $[\mathbf{4}\text{-}H_4]^+$ shows bond localization (Figure S1) as expected of an antiaromatic [4n]annulenoid system, demonstrated for instance for the 20-π-electron structure of germanium(IV) isophlorin.[21] The C(21)—C(1) and C(10)—C(11) bond lengths measure 1.469(4) Å and 1.470(4) Å, respectively, indicating that the phenanthrene moiety is bound to the dipyrromethene unit through sp^2–sp^2 single bonds.[22]

The atypical {CCNN} core of $\mathbf{4}\text{-}H_3$, consisting of two carbon and two nitrogen donors, makes it a candidate to act as a macrocyclic ligand. In fact, heating a deoxygenated solution of $\mathbf{4}\text{-}H_3$ to reflux in triethylamine (TEA) with phosphorus(III) trichloride for 2 h followed by recrystallization from dichloromethane/methanol produced phosphorus(V) phenanthriporphyrin $\mathbf{4}\text{-}P(OMe)_2$ in 43% yield (Scheme 3). Previously an incorporation of a phosphorus(V) center into the {CNN} coordination core of carbaporphyrinoid has been reported for N-fused dihydrotelluraporphyrin.[23]

A phenanthrene motif built into a chelating ligand has been very rarely encountered.[24,25] Nevertheless, the binding component where the C(4) and C(5) carbon atoms of phenanthrene (where the numbers refer to "free" phenanthrene) are simultaneously bound has been recognized in silylated phenanthrenes[26] and metalated triphenylene derivatives.[27–29]

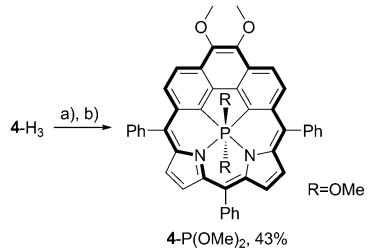

Scheme 3. Synthesis of $\mathbf{4}\text{-}P(OMe)_2$. Reaction conditions: a) PCl_3 (139 equiv), TEA, reflux, 2 h; b) CH_2Cl_2/MeOH, air.

The methoxide ligands at the phosphorus(V) center are readily exchangeable for hydroxides during chromatography on basic alumina or if traces of water are present in a solvent as documented by ^1H NMR spectroscopy (Figure S25). Consequently, it was crucial for any characterization that the sample was recrystallized just before measurements and that all experiments were carried out in an inert atmosphere.

The color of $\mathbf{4}\text{-}P(OMe)_2$ solutions in chlorinated solvents resembles that of $[\mathbf{4}\text{-}H_4]Cl$ which is directly reflected by the similarity of their UV/Vis electronic absorption spectra (Figure 1). The absorption spectrum of $\mathbf{4}\text{-}P(OMe)_2$ consists of three relatively narrow bands located at $\lambda = 388$ nm, 452 nm, and 480 nm supplemented by two broad and weak absorptions at $\lambda = 878$ nm and 962 nm.

Density functional theory (DFT) studies were used to visualize the proposed structures of $\mathbf{4}\text{-}H_3$ (Figure S34) and its phosphorus(V) complex to assess the degree of macrocycle distortion that is necessary to accommodate the phosphorus(V) cation. The geometry of $\mathbf{4}\text{-}P(OMe)_2$ (Figure 4) was

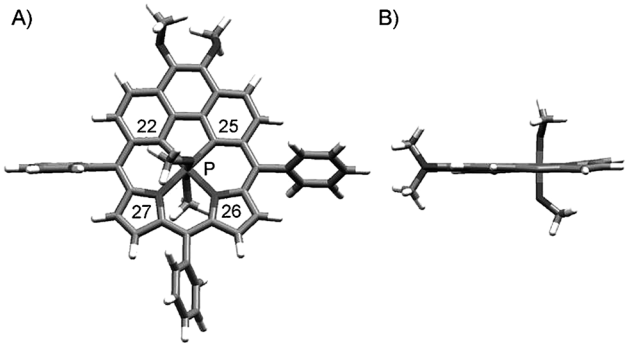

Figure 4. DFT (B3LYP/6-31G**) optimized model of $\mathbf{4}\text{-}P(OMe)_2$. Selected bond lengths [Å]: C(22)—P 1.900, C(25)—P 1.901, N(26)—P 1.963, N(27)—P 1.974.

optimized at the B3LYP/6-31G** level of theory, taking into consideration the coordination behavior of the phosphorus(V) atom in a reported porphyrinoid environment[30] and the geometric constraints imposed on the molecule, as indicated by a NOESY spectrum. In $\mathbf{4}\text{-}P(OMe)_2$, the phosphorus(V) atom is bound equatorially through two carbon and two nitrogen atoms. The coordination sphere is completed by two methoxide ligands. In fact the coordination

of phosphorus(V) was unambiguously confirmed using a combination of ^{1}H, ^{13}C, and ^{31}P NMR data.

Significantly, **4**-P(OMe)$_2$ conserves the paratropicity of **4**-H$_3$ as is reflected by the ^{1}H NMR spectrum which demonstrated a typical pattern for an antiaromatic porphyrinoid (Figure 5). Consistent with coordination, the signals attributable to H(22,25) and NH in **4**-H$_3$ disappear in the spectrum of **4**-P(OMe)$_2$. The doublet at $\delta = 6.63$ ppm assigned to methoxy ligands ($^{3}J_{P\text{-}H} = 21.2$ Hz) is relocated downfield as compared to trimethyl phosphate OP(OMe)$_3$ ($\delta = 3.78$ ppm) reflecting the paratropicity of **4**-P(OMe)$_2$. In the ^{31}P NMR spectrum, a ^{31}P resonance signal, attributable to the inserted phosphorus(V), appears at $\delta = -137.1$ ppm, a value which approaches the $\delta = -160$–-230 ppm range which is characteristic for phosphorus(V) porphyrins.[31] The ^{31}P NMR spectrum collected without ^{1}H decoupling showed a septet as a result of the coupling of the ^{31}P center with six equivalent protons of the two apical methoxy groups (Figure 5, inset B). In fact ^{31}P–^{1}H scalar coupling to all perimetric hydrogens have been detected in ^{1}H–^{31}P HMBC spectrum of **4**-P(OMe)$_2$ (Figure 5, inset A). The $^{1}J_{P\text{-}C(22,25)} = 167.2$ Hz scalar coupling constant explicitly confirms the presence of a P–C bond.

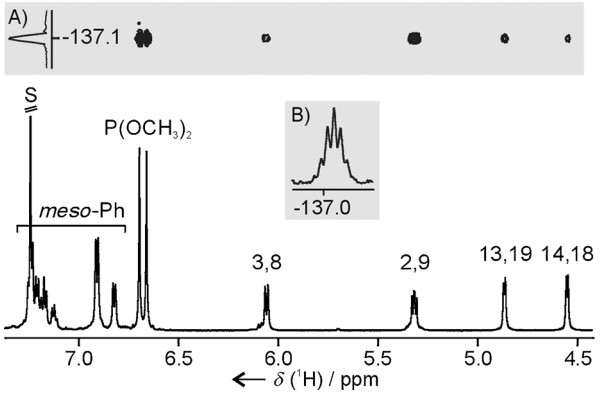

Figure 5. ^{1}H NMR spectrum of **4**-P(OMe)$_2$ (600 MHz, [D]chloroform, 220 K). Insets: A) ^{1}H–^{31}P HMBC map, B) ^{31}P NMR spectrum recorded without proton decoupling (250 MHz, [D]chloroform, 220 K).

^{1}H NMR chemical shifts have been calculated using the GIAO–B3LYP method for the optimized (B3LYP/6-31G**) geometries of paratropic **4**-H$_3$, [**4**-H$_4$]$^+$, and **4**-P(OMe)$_2$. There is a satisfactory qualitative agreement for each considered set of theoretical and experimental data demonstrated by linear correlations between the calculated and experimental chemical shifts (Figure S36–S38). Nucleus-independent chemical shift (NICS) values of the central 15-membered ring equal 12.1 (**4**-H$_3$) and 12.0 ([**4**-H$_4$]$^+$), consistent with the macrocyclic antiaromaticity of these systems.

To link together acenes and suitable porphyrinoids motifs, we employed a formal conversion of [18]tetraphyrin(1.1.1.0) through the hypothetical A,D-di-*m*-benziporphyrin(1.1.1.0) into phenanthriporphyrin—a hybrid macrocycle combining the structural features of polycyclic aromatic hydrocarbons and porphyrins. The nature of the connection between the two formal parts of the macrocycle results in its distinct antiaromatic character which is preserved after protonation. The unique coordination core of **4**-H$_3$ consists of two carbon and two nitrogen donors that can be activated toward coordination. Coordination is demonstrated by incorporation of a small cation to form the hypervalent organophosphorus derivative **4**-P(OMe)$_2$. Thus, phenanthriporphyrin can act as an antiaromatic, macrocyclic ligand, opening up exciting routes to explore coordination chemistry built on the specific reactivity of the phenanthrene unit.

Keywords: antiaromaticity · conjugation · phenanthrene · phosphorus · porphyrinoids

How to cite: *Angew. Chem. Int. Ed.* **2015**, *54*, 4932–4936
Angew. Chem. **2015**, *127*, 5014–5018

[1] M. Stępień, L. Latos-Grażyński, *J. Am. Chem. Soc.* **2002**, *124*, 3838–3839.
[2] T. D. Lash, A. M. Toney, K. M. Castans, G. M. Ferrence, *J. Org. Chem.* **2013**, *78*, 9143–9152.
[3] M. Stępień, L. Latos-Grażyński, L. Szterenberg, *J. Org. Chem.* **2007**, *72*, 2259–2270.
[4] C. H. Hung, C. Y. Lin, P. Y. Lin, Y. J. Chen, *Tetrahedron Lett.* **2004**, *45*, 129–132.
[5] T. D. Lash, A. M. Young, J. M. Rasmussen, G. M. Ferrence, *J. Org. Chem.* **2011**, *76*, 5636–5651.
[6] B. Szyszko, L. Latos-Grażyński, *Organometallics* **2011**, *30*, 4354–4363.
[7] B. Szyszko, L. Latos-Grażyński, L. Szterenberg, *Chem. Commun.* **2012**, *48*, 5004–5006.
[8] B. Szyszko, E. Pacholska-Dudziak, L. Latos-Grażyński, *J. Org. Chem.* **2013**, *78*, 5090–5095.
[9] S.-D. Jeong, K. J. Park, H.-J. Kim, C.-H. Lee, *Chem. Commun.* **2009**, 5877–5879.
[10] M. Pawlicki, L. Latos-Grażyński in *Handbook of Porphyrin Science: with Applications to Chemistry, Physics, Materials Science Engineering, Biology and Medicine*, *Vol. 2* (Eds.: K. M. Kadish, K. M. Smith, R. Guilard), World Scientific Publishing, Singapore, **2010**, 104–192.
[11] B. Szyszko, L. Latos-Grażyński, L. Szterenberg, *Angew. Chem. Int. Ed.* **2011**, *50*, 6587–6591; *Angew. Chem.* **2011**, *123*, 6717–6721.
[12] B. Szyszko, K. Kupietz, L. Szterenberg, L. Latos-Grażyński, *Chem. Eur. J.* **2014**, *20*, 1376–1382.
[13] D. I. AbuSalim, G. M. Ferrence, T. D. Lash, *J. Am. Chem. Soc.* **2014**, *136*, 6763–6772.
[14] H. Furuta, H. Maeda, A. Osuka, *J. Am. Chem. Soc.* **2000**, *122*, 803–807.
[15] M. Stępień, B. Szyszko, L. Latos-Grażyński, *Org. Lett.* **2009**, *11*, 3930–3933.
[16] J. S. Lindsey, I. C. Schreiman, H. C. Hsu, P. C. Kearney, A. M. Marguerettaz, *J. Org. Chem.* **1987**, *52*, 827–836.
[17] M. Ishida, Y. Naruta, F. Tani, *Angew. Chem. Int. Ed.* **2010**, *49*, 91–94; *Angew. Chem.* **2010**, *122*, 95–98.
[18] Crystal data for [**4**-H$_4$]Cl are given in the Supporting Information. CCDC 1043900 contains the supplementary crystallographic data for this paper. These data can be obtained free of charge from The Cambridge Crystallographic Data Centre via www.ccdc.cam.ac.uk/data_request/cif.
[19] J. L. Sessler, S. J. Weghorn, *Expanded, Contracted, and Isomeric Porphyrins* (Eds.: J. E. Baldwin, P. D. Magnus), Elsevier Science, Oxford, **1997**.
[20] F. Calderazzo, C. Forte, F. Marchetti, G. Pampaloni, L. Pieretti, *Helv. Chim. Acta* **2004**, *87*, 781–789.

[21] J. A. Cissell, T. P. Vaid, G. P. A. Yap, *J. Am. Chem. Soc.* **2007**, *129*, 7841 – 7847.
[22] A. M. Shachter, E. B. Fleisher, C. Haltiwanger, *Acta Crystallogr. Sect. C* **1987**, *43*, 1876 – 1878.
[23] E. Pacholska-Dudziak, F. Ulatowski, Z. Ciunik, L. Latos-Grażyński, *Chem. Eur. J.* **2009**, *15*, 10924 – 10929.
[24] N. Das, P. J. Stang, A. M. Arif, C. F. Campana, *J. Org. Chem.* **2005**, *70*, 10440 – 10446.
[25] D. C. Flynn, G. Ramakrishna, H.-B. Yang, B. H. Northtop, P. J. Stang, T. Goodson III, *J. Am. Chem. Soc.* **2010**, *132*, 1348 – 1358.
[26] M. Oba, M. Iida, T. Nagoya, K. Nishiyama, *J. Organomet. Chem.* **2006**, *691*, 1151 – 1153.
[27] R. Ara Begum, N. Chanda, T. V. V. Ramakrishna, P. R. Sharp, *J. Am. Chem. Soc.* **2005**, *127*, 13494 – 13495.
[28] N. Chanda, P. R. Sharp, *Organometallics* **2007**, *26*, 1635 – 1642.
[29] T. V. V. Ramakrishna, P. R. Sharp, *Organometallics* **2004**, *24*, 3079 – 3081.
[30] S. Mangani, E. F. Meyer, D. L. Cullen, M. Tsutsui, C. J. Carrano, *Inorg. Chem.* **1983**, *22*, 400 – 404.
[31] T. Barbour, W. J. Belcher, P. J. Brothers, C. E. F. Rickard, C. J. Ware, *Inorg. Chem.* **1992**, *31*, 746 – 754.
[32] K. Paruch, L. Vyklický, T. J. Katz, *Org. Synth.* **2003**, 227 – 232.

Received: January 26, 2015
Published online: February 26, 2015